Biosensors and Bioelectronics 213 (2022) 114458

Contents lists available at ScienceDirect

Biosensors and Bioelectronics

journal homepage: www.elsevier.com/locate/bios

# Power-free microfluidic biosensing of *Salmonella* with slide multivalve and disposable syringe

Ruya Guo [a], Li Xue [b,1], Nana Jin [a], Hong Duan [a], Miaoyun Li [c], Jianhan Lin [b,*]

[a] Key Laboratory of Agricultural Information Acquisition Technology, Ministry of Agriculture and Rural Affairs, China Agricultural University, Beijing, 100083, China
[b] Key Laboratory of Smart Agriculture System Integration Research, Ministry of Education, China Agricultural University, Beijing, 100083, China
[c] College of Food Science and Technology, Henan Agricultural University, Zhengzhou, 450002, China

ARTICLE INFO

*Keywords:*
Microfluidic biosensor
Power-free detection
Slide multivalve
Disposable syringe
*Salmonella*

ABSTRACT

In this study, a power-free biosensor was presented to detect *Salmonella* typhimurium on a microfluidic chip using a slide multivalve for channel selection and a disposable syringe for fluidic transfer. First, bacterial sample with immunomagnetic nanoparticles (IMNPs) and glucose oxidase (GOx) modified immune polystyrene nanoparticles (IPNPs), washing buffer, glucose, and peroxide test strip (PTS) were preloaded in their respective chambers at the periphery of chip. After the slide multivalve was selected to connect sample chamber with common separation chamber, which was connected with a syringe, the mixture of *Salmonella*, IMNPs and IPNPs was back and forth moved through 3D Tesla-structure micromixer using the syringe, resulting in the formation of IMNP-*Salmonella*-IPNP complexes, which were captured in the separation chamber using a magnet. Then, two washing chambers were selectively connected respectively to remove sample background and excessive IPNPs, and glucose chamber was connected, allowing the GOx to catalyze glucose to produce hydrogen peroxide in the separation chamber. Finally, PTS chamber was connected and the catalysate was transferred from the separation chamber to the PTS chamber, leading to the color change of PTS, followed by using smartphone App to collect and analyze the image of PTS for bacterial determination. The simple biosensor enabled simple detection of *Salmonella* as few as 130 CFU/mL within 60 min and is promising for practical applications in the resource-limited regions due to its low cost, simple operation, and small size.

## 1. Introduction

As a major foodborne pathogen, *Salmonella* has increasingly attracted global concern because it can contaminate foods at any link of their supply chains and trigger foodborne diseases such as diarrhea, typhoid fever, and even death. Early screening of *Salmonella* has been a key to prevent and control the outbreaks of some foodborne diseases. Currently, available methods for detecting *Salmonella* mainly include culture plating (Iseri et al. 2020), polymerase chain reaction (PCR) (Meng et al. 2017), and enzyme linked immunosorbent assay (ELISA) (Um et al. 2020). Culture is the gold standard method with high sensitivity and accuracy, however it usually takes 2–3 days. PCR and ELISA are the recommended rapid methods, however they require complex pretreatment (PCR) or lack enough sensitivity (ELISA). Hence, rapid, simple and sensitive methods are demanded for *Salmonella* detection to ensure food safety.

With rapid advances of microfluidics, a variety of microfluidic biosensors were developed as an alternative for bacterial detection in the past decade due to their integration of complex procedures from sample loading to result analysis onto a chip (Xing et al. 2021). Prior to bacterial detection, immunomagnetic separation with immunomagnetic particles has been usually employed to specifically isolate target bacteria from the complex food matrix (Wang et al. 2020). Recently, many efforts have been made on the development of microfluidic biosensors with immunomagnetic separation (Hussain et al. 2022; Kim and Choi, 2020; Ting-Hang et al., 2019). An interesting microfluidic biosensor was reported for HIV-1 p24 detection by integrating multi-step reactions onto a chip (Liu et al. 2020). A permanent magnet was used to move magnetic particles from one chamber to another, which were separated by an oil barrier. It enabled sensitive and reliable detection of HIV-1 p24 as low as 0.5 ng/mL within 1 h. However, the transfer of magnetic particles through the oil barrier might lead to their partial loss in the oil. Besides,

* Corresponding author.
*E-mail address:* jianhan@cau.edu.cn (J. Lin).
[1] This author makes the equal contribution with the first author.

https://doi.org/10.1016/j.bios.2022.114458
Received 13 April 2022; Received in revised form 30 May 2022; Accepted 5 June 2022
Available online 7 June 2022

precise fluidic control is crucial for microfluidic biosensors, which is often achieved using peristaltic pumps or injection pumps and valves. However, most of them might not be applicable for in-field screening of foodborne bacteria since they were usually expensive, bulky and dependent on external electrical power. More importantly, they often suffered from cross contaminations and thus resulted in potential false positives. To overcome these issues, some finger-actuated (Park et al. 2020; Park and Park, 2019), capillary-driven (Rocca et al. 2021; Yakoh et al. 2019) and magnetic-adhesive (Harper et al. 2016) pumps and valves were developed and demonstrated with no need of electrical power and controller. However, they also had some limitations, such as narrow flowrate range and uncontrollable fluidic operation. As an alternative, a slide valve based on rigid or semi-rigid walls was proposed and verified to reversibly open and close a channel without any external equipment and power (Venzac et al. 2020). In addition, micromixer is a key to a microfluidic chip and various micromixers have been often reported with excellent mixing efficiency (Bayareh et al. 2020; Cai et al. 2017; Lee and Fu, 2018; Raza et al. 2020). Among them, the 3D Tesla-structure micromixer showed an outstanding mixing performance over a wide range of Reynolds numbers, indicating that it was applicable for wide flowrate range (Yang et al. 2015). Very recently, a reciprocating-flow immunobinding strategy was proposed using a water bottle to achieve adequate antibody-antigen immunobinding within 60 s due to continuous contact between antibodies and antigens (Liu et al. 2021). Thus, integration of slide valve, 3D Tesla-structure micromixer and reciprocating-flow immunobinding strategy might pave a prospective way to develop power-free microfluidic chips for immunological detection of bacteria.

To achieve in-field screening of pathogenic bacteria, some simple and low-cost methods based on test papers and strips have been successfully developed and integrated with microfluidic chips (Ming et al. 2020; Nishat et al. 2021; Zhang et al.). A typical study on the combination of a microfluidic chip with a #1 chromatography paper and mixed-dye-loaded loop-mediated isothermal amplification assay was conducted for multiplex foodborne pathogen detection with a detection limit of $10^3$ CFU/mL (Pang et al. 2018). Like common pH test paper, peroxide test strip is often used to rapidly measure various peroxides, such as $H_2O_2$, and featured with facile size, low cost, and fast response. More importantly, the resulting color, which is related with the concentration of peroxide, could be easily measured using a smartphone App (Liu et al. 2019) or the Image J software. Thus, it is very promising to combine microfluidic chip, peroxide test strip and smartphone image processing to develop power-free, easy-operation, low-cost and rapid-response biosensors for in-field screening of pathogenic bacteria.

Here, a power-free microfluidic biosensor was proposed to detect *Salmonella* based on slide valve, disposable syringe, and smartphone. As shown in Fig. 1, this biosensor was mainly composed of a five-layer microfluidic chip with a slide multivalve and a disposable syringe. First, the bacterial sample with the immunomagnetic nanoparticles (IMNPs) and glucose oxidase (GOx) modified immune polystyrene nanoparticles (IPNPs), washing buffer, glucose, and peroxide test strip (PTS) were preloaded in the peripheric sample chamber, washing chambers, glucose chamber and PTS chamber, respectively. Then, the sample chamber was connected with the common separation chamber by rotating the slide multivalve, the mixture was moved back and forth to flow through the 3D Tesla-structure micromixer by using a disposable syringe, resulting in the formation of IMNP-*Salmonella*-IPNP sandwich complexes, which were captured in the separation chamber by applying a magnet. Then, the washing chambers were successively connected respectively to remove excessive IPNPs, and the glucose chamber was connected to transfer glucose to suspend the complexes in the separation chamber, allowing the GOx on the complexes to catalyze glucose to produce hydrogen peroxide ($H_2O_2$). Finally, the PTS chamber was connected and the catalysate in the separation chamber was transferred

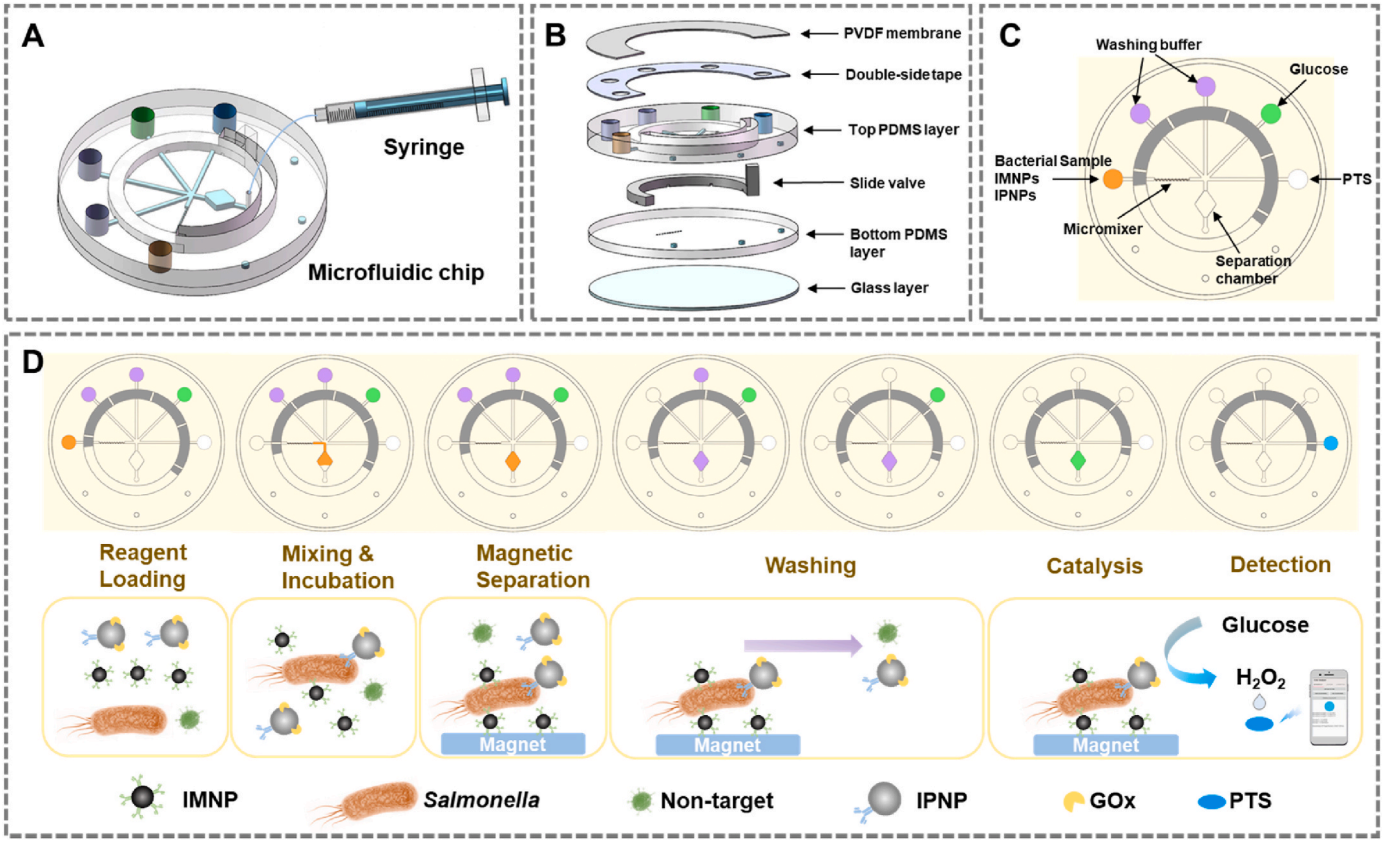


**Fig. 1.** Principle of the power-free microfluidic biosensor for *Salmonella* detection. (A) The 3D design of microfluidic chip; (B) The layer-by-layer structure of microfluidic chip; (C) The top view of microfluidic chip; (D) The procedures for *Salmonella* detection.

to the PTS chamber, leading to the color change of the PTS, followed by using the smartphone App to collect and analyze its image to determine the amount of *Salmonella*.

## 2. Materials and methods

### 2.1. Materials

The information for materials and reagents, such as carboxylated magnetic nanoparticles (MNPs), carboxylated polystyrene nanoparticles (PNPs), monoclonal and polyclonal antibodies against *Salmonella*, glucose oxidase, glucose, peroxide test strips, etc., could be found in the supplemental material.

### 2.2. Preparation of the bacterial strains

The culture and preparation of the target and non-target bacteria for obtaining a serial dilution of bacterial samples could be found in the supplemental material.

### 2.3. Preparation of the IMNPs and IPNPs

The IMNPs were prepared by modifying the polyclonal antibodies onto the carboxylated MNPs and the detailed procedure could be found in the supplemental material. The IPNPs were prepared through EDC/NHS method to modify the monoclonal antibodies and glucose oxidases onto the carboxylated PNPs based on previous report with some modifications (Chen et al. 2017). First, 0.2 mg of PNPs were centrifuged at 12,000 rpm for 10 min to remove the supernatant, and resuspended with 2.5 mL of phosphate buffer (PB, pH 6.0, 10 mM). After 0.1 mg of monoclonal antibodies and 0.1 mg of GOx were successively added and incubated for 60 min under gentle stirring, 30 μg of EDC·HCl was immediately added and incubated for 60 min, followed by blocking with 1% skim milk for 60 min and centrifugation at 12,000 rpm for 10 min. Finally, the IPNPs were resuspended in 0.4 mL of PBS (containing 1% skim milk) and stored at 4 °C.

### 2.4. Fabrication of the microfluidic chip

This microfluidic chip was fabricated to integrate the whole bacterial detection procedures, including mixing, incubation, separation, washing, catalysis and detection. From Fig. 1B, the microfluidic chip consisted of a PVDF membrane (inner diameter: 44 mm, outer diameter: 70 mm), a double-side tape (inner diameter: 44 mm, outer diameter: 70 mm), a top PDMS layer (diameter:70 mm, thickness: 5 mm), a slide multivalve (inner diameter: 35.8 mm, outer diameter: 44.2 mm, thickness: 3.2 mm), a bottom PDMS layer (diameter: 70 mm, thickness: 3 mm), and a glass layer (diameter: 70 mm, thickness: 1 mm). The PVDF membrane was water-proof to avoid the loss of the reagents and also air-permeable to allow the transfer of the reagents. The double-side tape with five circular holes (diameter:6 mm) was used to bond the PVDF membrane and the PDMS layer. The slide multivalve with different intervals of five connecting channels (length: 4.2 mm, width: 0.8 mm, height: 0.7 mm) was used to clockwise connect each chamber with the separation chamber one by one. The top PDMS layer with one half 3D Tesla-structure micromixer and same interval of five channels (width: 1 mm, height: 0.8 mm) and the bottom PDMS layer with the other half 3D Tesla-structure micromixer were surface plasmon bonded to form the fluidic channels and the complete micromixer. The different interval of the channels in slide multivalve and the same interval of the channels in PDMS channel enabled the connection of only one peripheric chamber with the inner separation chamber. From Fig. 1C, this chip mainly included five peripheric circle chambers (diameter: 6 mm, height: 5 mm, volume: ~140 μL) for preloading the sample with IMNPs and IPNPs, washing buffers, glucose and PTS, one inner diamond separation chamber (volume: ~100 μL) for separating the complexes, washing the residues and catalyzing the substrate, and one 3D Tesla-structure micromixer for mixing the bacterial sample with the IMNPs and IPNPs. Besides, three convex and concave structures were used for accurate alignment of these two PDMS layers, and a PTS circle disk (diameter: 5.0 mm) was cut using a hand-held puncher chamber and placed in the PTS chamber before the bonding of the PDMS layers. The slide valve was first designed using SolidWorks software, then fabricated using the Object30 Pro 3D printer, and finally inserted into the gap of the chip after coating with a thin layer of silicone oil. Besides, the molds of the PDMS layers were first fabricated using this 3D printer, then casted by the mixture of PDMS prepolymer and curing agent (10:1 in mass), and finally cured at 65 °C overnight after degassing in vacuum to obtain the PDMS layers.

### 2.5. Detection of Salmonella

Prior to test, the microfluidic chip was preloaded with 100 μL of washing buffer (PBST, PBS containing 0.05% Tween-20) in each washing chamber, 100 μL of glucose (50 mM) in glucose chamber and a PTS disk in PTS chamber, and the separation chamber was blocked by 1% skim milk for 1 h and washed by sterile PBS. As shown in Figs. 1D and 100 μL of the bacterial sample at each concentration ($1.3 \times 10^2$–$1.3 \times 10^7$ CFU/mL), 10 μL of the IMNPs (20 μg) and 10 μL of the IPNPs (10 μg) were added into the sample chamber before the slide valve was connected. First, the sample chamber was connected, the mixture was pulled and pushed using a disposable syringe to flow through the 3D Tesla-structure micromixer back and forth for ten times, resulting in the formation of IMNP-*Salmonella*-IPNP sandwich complexes. Then, these complexes were captured in the separation chamber using an external magnet (material: NdFeB, grade: N52, size: 3.18 × 6.36 × 6.36 mm), and two washing chambers were successively connected to wash the complexes with washing buffer to remove excessive IPNPs. After the glucose chamber was connected, 100 μL of glucose was moved to the separation chamber, allowing the GOx on the complexes to catalyze glucose for 30 min to produce $H_2O_2$ in the catalysate. Finally, the PTS chamber was connected and the catalysate in the separation chamber was transferred to the PTS chamber, leading to the color change of the PTS, which was collected and analyzed using the self-developed smartphone App (Fig. S1) to determine the target bacteria.

## 3. Results and discussion

### 3.1. Sealing of the slide multivalve

In this microfluidic chip, a ring-shaped rigid-structure resin wall with different intervals of channels was used as the slide multivalve, which was tightly matched with the ring-shaped semi-rigid-structure PDMS gap to selectively connect each peripheric channel with the common separation channel. To ensure the sealing of the chip, silicone oil was used to coat the surface of the slide valve for lubrication and sealing, and the size of the slide valve was optimized. When each size of slide valve was coated with silicone oil, inserted into the PDMS gap with inner diameter (Di) of 36 mm, outer diameter (Do) of 44 mm and thickness of 3 mm, and set at disconnection with the washing chamber, where the red dye was preloaded, the syringe was used to fully draw the red dye for evaluating the sealing. As shown in Fig. 2 and Videos S1–S3, the air bubbles obviously appeared at the same size of Di = 36.0 mm and Do = 44.0 mm with the gap and the larger size of Di = 35.9 mm and Do = 44.1 mm than the gap, when the slide valve was connected with the separation chamber and the red dye was fully drawn using the syringe, indicating the sealing of this slide valve was not good. When a further larger size of Di = 35.8 mm and Do = 44.2 mm was used for the slide valve, the syringe was hard to draw the red dye and no air bubble occurred, indicating the sealing of the valve was good enough. Thus, Di = 35.8 mm and Do = 44.2 mm were used for this slide valve. To further verify the feasibility of this slide valve, different colors of dyes were

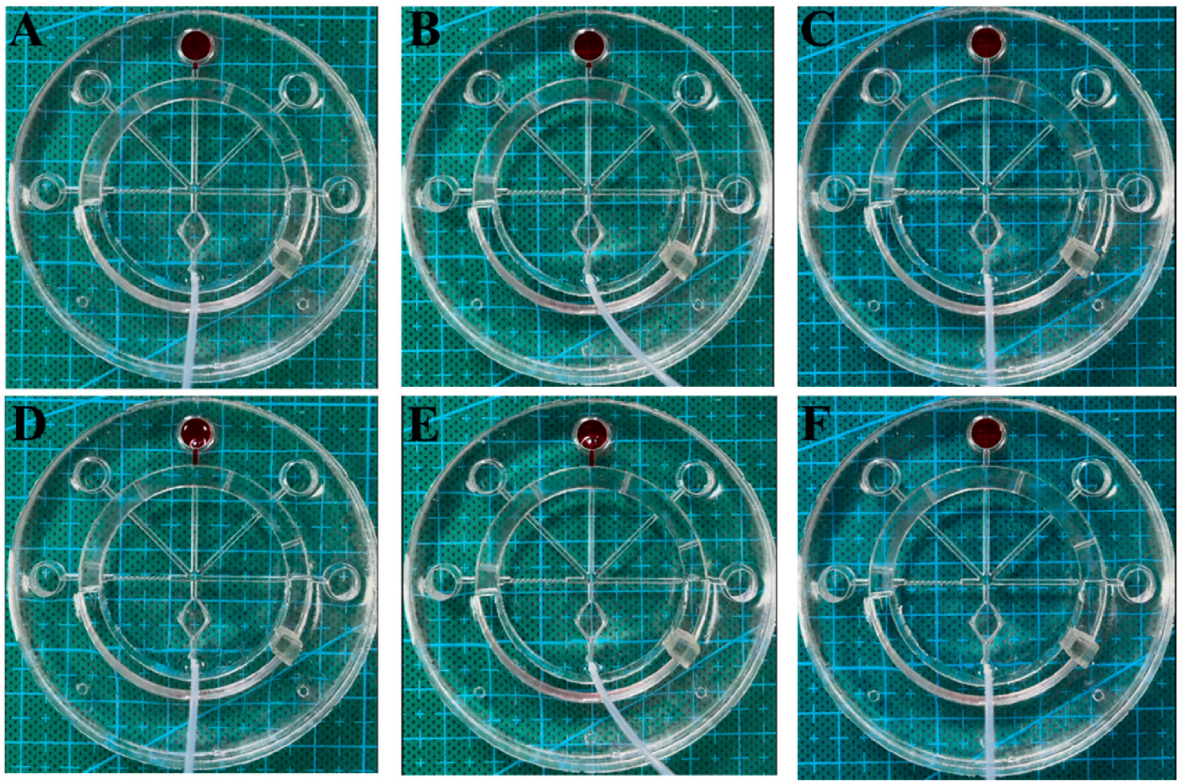


**Fig. 2.** The sealing of the slide valves with different sizes before (A, B, C) and after (D, E, F) drawing the dye using the syringe. (A and D: Di = 36.0 mm and Do = 44.0 mm; B and E: Di = 35.9 mm and Do = 44.1 mm; C and F: Di = 35.8 mm and Do = 44.2 mm).

preloaded in the chambers and drawn one-by-one using the syringe. As shown in **Video S4**, the dyes were completely drawn into the separation chamber when their chambers were connected one-by-one, indicating the good feasibility of this valve.

Supplementary data related to this article can be found at https://doi.org/10.1016/j.bios.2022.114458.

### 3.2. Performance of the 3D Tesla-structured micromixer

The mixing of target bacteria with the IMNPs and IPNPs basically relied on the 3D Tesla-structure micromixer, which is crucial to the sensitivity of this biosensor. Thus, COMSOL software was used to simulate this 3D Tesla-structure micromixer and the mixing efficiency was used to evaluate its performance. As shown in Fig. 3A and Fig. S2A, this micromixer showed a good mixing efficiency of up to 96%. To evaluate the actual mixing performance of this micromixer, a red dye and water were injected into the micromixer at the same time and the images at the inlet and outlet were collected using the microscope (Ti-E, Nikon, Tokyo, Japan). As shown in Fig. 3B, the dye was obviously separate from the water at the inlet, and they were well mixed at the outlet since the color looked uniform. Besides, the images were further analyzed by the ImageJ software. From Fig. S2B, the gray values exhibited two levels at the inlet while they tended to be uniform at the outlet, indicating good mixing performance of this micromixer.

To further evaluate the performance of this micromixer on immunobinding, the IMNPs and the bacterial sample were first added into the sample chamber with this micromixer, respectively. The same IMNPs and sample were added into the symmetric PTS chamber without this micromixer (straight channel) and PTS disk for comparison, and the same IMNPs and sample were also added into the washing chamber without any operation for control. Then, their mixture was moved back and forth for ten times using the syringe to form magnetic bacteria. After the magnetic bacteria were captured in the separation chamber using the magnet and the unbound bacteria were removed, the captured bacteria were finally flushed out and culture plated to determine the captured bacteria. The capture efficiency was defined as the ratio of the captured bacteria to the original one. As shown in Fig. 3C, the capture efficiency with the 3D Tesla-structure micromixer (91%) was much higher than that with the straight channel (56%) and that without any operation (26%), indicating its good performance on the immunobinding of the IMNPs and target bacteria. This might be due to the good mixing performance of this micromixer and the continuous contact from repeated reciprocating-flow, which resulted in increasing collision probability between the IMNPs and target bacteria.

The time for the syringe to move the mixture back and forth is important for the mixing performance on immunobinding. Thus, different times were applied to mix the IMNPs and bacterial sample ($1.3 \times 10^3$ CFU/mL). From Fig. 3D, as the times changed from 3 to 10, the capture efficiency increased from 56% to 91%. However, further increase on the time to 15 only resulted in slight increase on the capture efficiency. Therefore, ten times of moving the mixture were used. To realize the power-free detection, the disposable syringe was used to replace the precise pump, and this might result in difficult control on the flowrate. Thus, different flowrates controlled by using a precise peristaltic pump (Type: T60-S2 & WX10-14-A, Longer Pump, Baoding, China) were used to mix the mixture. From Fig. 3E, the capture efficiency basically remained more than 80%, when the flowrate increased from 0.5 to 1.25 mL/min, which was easy to control by manual operation. To further evaluate the difference on manual operation, three graduate students were minimally trained to conduct the test. As shown in Fig. 3F, the capture efficiency of the three students were all above 80%, indicating the good practicability of this chip.

### 3.3. Concept proof of the detection method and optimization of the parameters

The determination of target bacteria was based on the catalysis of glucose by the GOx on the complexes to produce $H_2O_2$ and the image

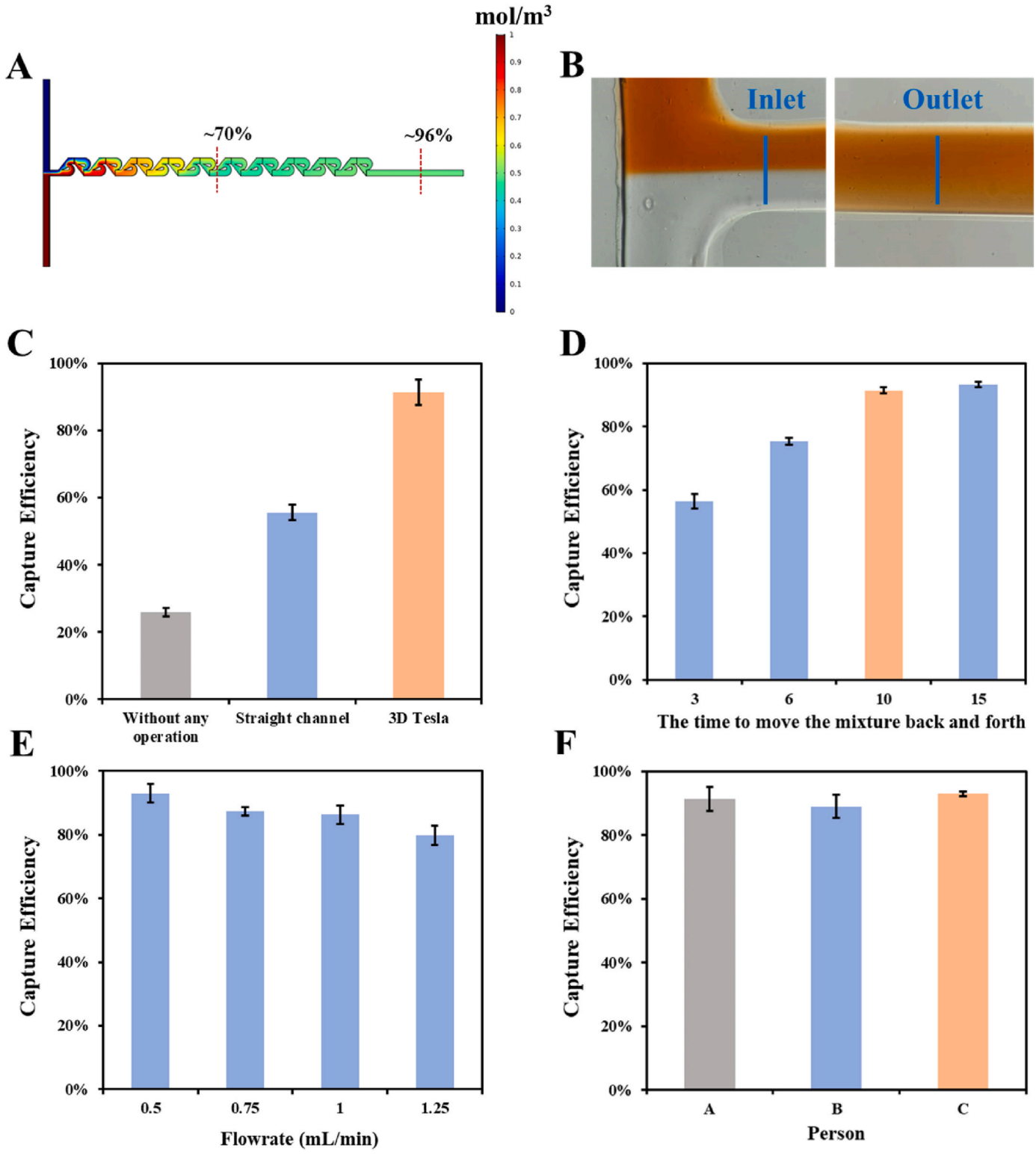


**Fig. 3.** (A) The COMSOL simulation result of the 3D Tesla-structure micromixer; (B) The images of the mixture of red dye and water at the inlet and outlet; (C) The comparison on the capture efficiency of target bacteria with the 3D Tesla-structure micromixer, with the straight channel and without any operation (N = 3); (D) The optimization of the time for the syringe to move the mixture back and forth (N = 3); (E) The capture efficiency for different flowrates (N = 3); (F) The capture efficiency for different persons (N = 3).

analysis of the PTS. To prove the concept, different concentrations of the IPNPs from 0 to 500 μg/mL were used to react with 100 μL of glucose (50 mM) for 30 min and 10 μL of the catalysate was added to the PTS. From Fig. 4A, the blue color of the PTSs changed from light to dark as the concentration increased. The images of the PTSs were further analyzed to obtain their saturation using the self-developed smartphone App. From Fig. 4B, the saturation increased with the concentration of IPNPs. From Fig. 4C, a linear model between saturation and IPNP concentration (3.91–500 μg/mL) was found, verifying the feasibility of this concept.

To evaluate the loading capacity of IPNPs, different amounts of

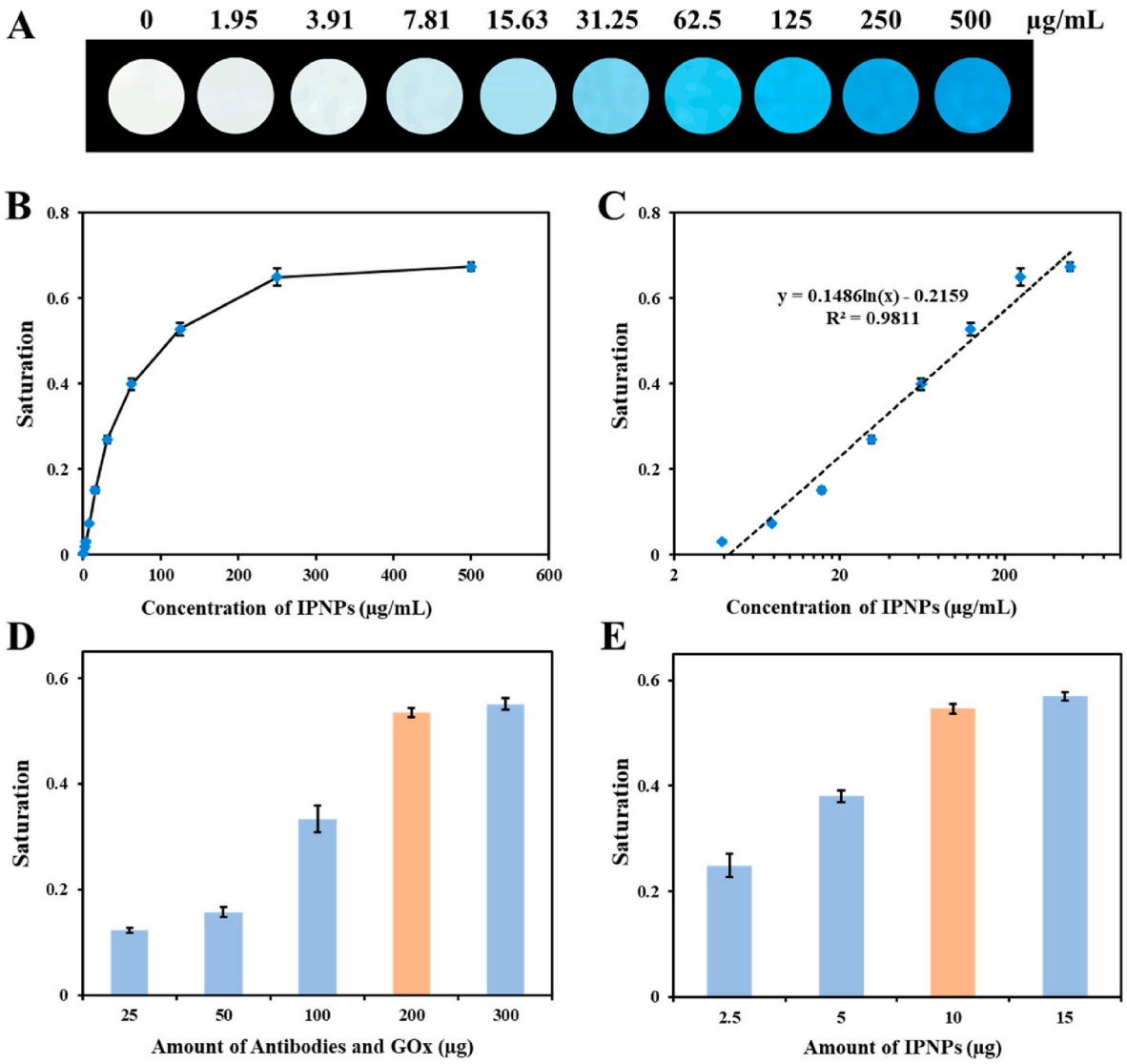


**Fig. 4.** (A) The color change of the strips for different concentrations of IPNPs from 0 to 500 μg/mL; (B) The saturation of the strips for different concentrations of IPNPs from 0 to 500 μg/mL (N = 3); (C)The linear model between saturation and IPNP concentration from 3.91 to 500 μg/mL (N = 3); (D) Optimization of the amount of antibodies and GOx (N = 3); (E) Optimization of the amount of IPNPs (N = 3).

antibodies and GOx with the ratio of 1:1 from 25 to 300 μg were used to prepare the IPNPs for detection of *Salmonella* at $1.3 \times 10^6$ CFU/mL. From Fig. 4D, the saturation changed from 0.12 to 0.54 as the amount increased from 25 to 200 μg. However, further increase to 300 μg did not lead to obviously more increase on the saturation, indicating that 200 μg was sufficient to prepare the IPNPs. Besides, the amount of IPNPs for bacterial labeling is also vital to this biosensor. Thus, different amounts of IPNPs from 2.5 to 15 μg were used to detect *Salmonella* at $1.3 \times 10^6$ CFU/mL. From Fig. 4E, the saturation changed from 0.25 to 0.55 as the amount increased from 2.5 to 10 μg. Only slight increase on the saturation was observed when the amount further increased to 15 μg. Thus, 10 μg of IPNPs were used.

### 3.4. Performance of the biosensor

To establish the model of this biosensor, different concentrations of *Salmonella* from $1.3 \times 10^2$ to $1.3 \times 10^7$ CFU/mL were detected. From Fig. 5A, a visible color change of the PST was observed, and the saturation increased from 0.12 to 0.58 as the concentration of *Salmonella* changed from $1.3 \times 10^2$ to $1.3 \times 10^7$ CFU/mL. From Fig. 5B, a linear model between saturation (***S***) and bacterial concentration (***C***) was observed and expressed as $\boldsymbol{S} = 0.1177 \log(\boldsymbol{C}) - 0.1633$ ($R^2 = 0.9743$). The detection limit of the biosensor was determined to be 130 CFU/mL. Compared to some recently reported methods for bacteria detection in Table S1, this biosensor exhibited good performance with higher detection sensitivity or shorter detection time. This may be attribute to the following aspects: (1) the 3D Tesla-structure micromixer with repeated reciprocating-flow was employed to greatly improve the antigen-antibody immunobinding, resulting in the forming of more sandwich complexes; (2) the IPNPs with GOx were used to effectively amplify the biological signals, resulting in the detectable signal for low concentrations; (3) the smartphone App was developed to accurately measure the color change of the PTS, resulting in high signal-to-noise ratio. More importantly, this biosensor was able to carry out the whole bacterial detection procedure on this microfluidic chip within 60 min, and it only costed ~$20.7 (See Table S2). Besides, transmission electron microscopy was conducted to confirm the forming of IMNP-*Salmonella*-IPNP sandwich complexes (Fig. 5C).

To evaluate the specificity of this biosensor, the negative control (PBS), the target bacteria (*Salmonella* typhimurium) at $1.3 \times 10^5$ CFU/mL, five non-target bacteria (*E. coli* O157:H7, *Listeria monocytogenes, Staphylococcus aureus, Vibrio parahaemolyticus,* and *Bacillus cereus*) at

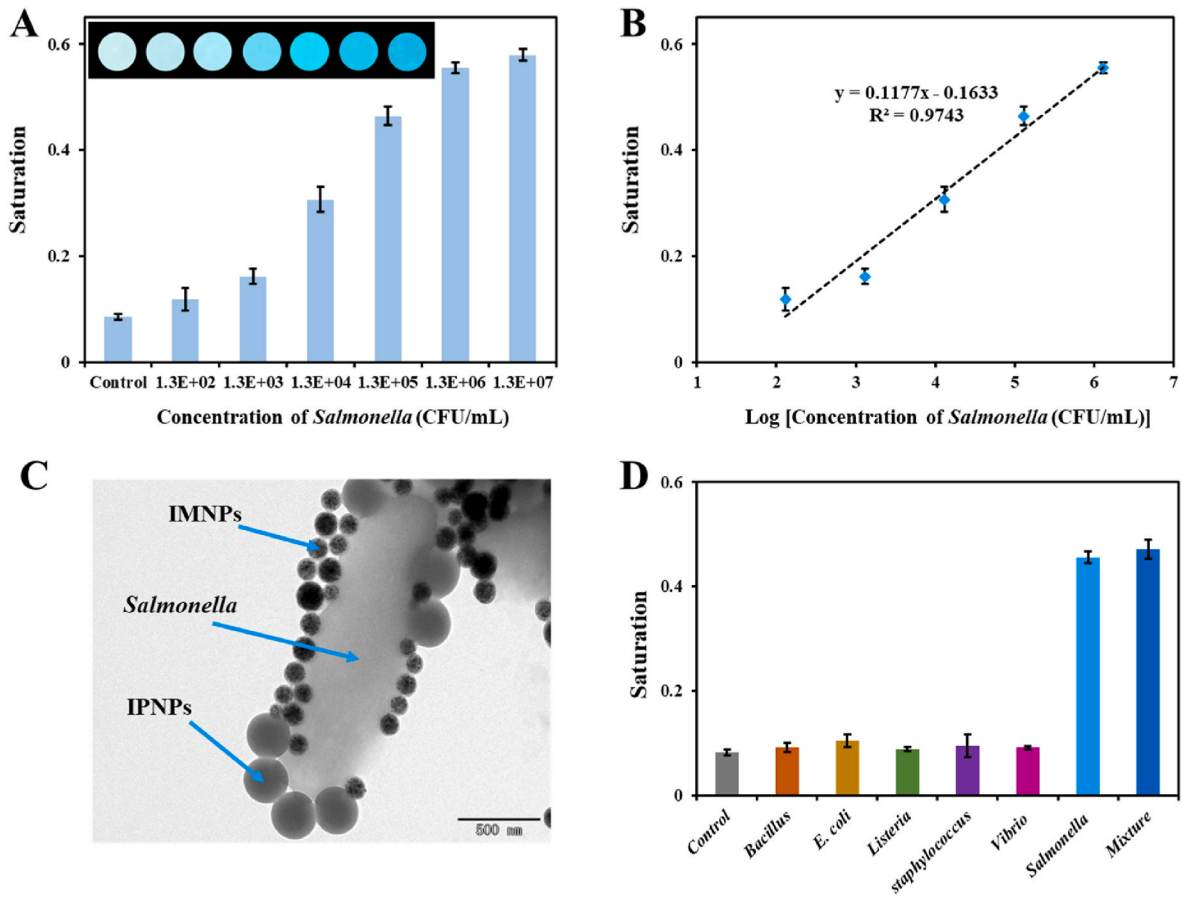


**Fig. 5.** (A) The saturation for different concentrations of *Salmonella* (N = 3); (B) Calibration model of the biosensor (N = 3); (C) The TEM image of IMNP-*Salmonella*-IPNP sandwich complex; (D) The specificity of the biosensor (N = 3).

$10^5$ CFU/mL and their mixture were all detected by this biosensor. As shown in Fig. 5D, the saturation for the target bacteria and the mixture was obviously higher than those for non-target bacteria and negative control, verifying a good specificity of the biosensor.

The applicability of this biosensor was also estimated by detecting the chicken meat samples spiked with *Salmonella* from $1.4 \times 10^2$ CFU/mL to $1.4 \times 10^5$ CFU/mL, which were determined using the gold standard culture plating method. After 25 g of chicken meat was first homogenized with 225 mL of sterile PBS for 5 min, followed by standing for 10 min to obtain the supernatant, different concentrations of *Salmonella* were added into the supernatant to prepare the spiked samples, which were detected using this biosensor. As shown is Table 1, the recoveries for $1.4 \times 10^2$ CFU/mL to $1.4 \times 10^5$ CFU/mL were 122.9%, 80.3%, 105.6% and 98.6%, respectively, indicating the impurities in chicken meats, such as fats and proteins, had certain impact on the separation of target bacteria and resulted in higher or lower concentrations from the biosensor. The higher concentration was probably resulted from the non-specific reaction between the IMNPs and few impurities, while the lower concentration was probably because the impurities became a hindrance to the immunobinding of the IMNPs with target bacteria.

**Table 1**
The recovery of *Salmonella* in spiked chicken samples (N = 3).

| Spiked concentration (CFU/mL) | Detected concentration (CFU/mL) | Recovery (%) | RSD (%) |
|---|---|---|---|
| **140** | **172** | **122.9** | **15.5** |
| **1400** | **1124** | **80.3** | **12.9** |
| **14000** | **14788** | **105.6** | **6.1** |
| **140000** | **138008** | **98.6** | **5.3** |

## 4. Conclusions

In summary, a power-free microfluidic biosensor based on slide multivalve and disposable syringe was successfully developed and demonstrated with the capability to detect *Salmonella* as low as 130 CFU/mL within 1 h. The slide multivalve was verified with good sealing and could be used to easily select the desired channels. The combination of the 3D Tesla-structure micromixer and repeated reciprocating-flow using the disposable syringe was proved with good mixing effect for antigen-antibody immunobinding. More importantly, this biosensor could quantitatively determine target bacteria by simply operating the microfluidic chip, and has shown the potential for in-field screening of foodborne bacteria. However, the drawbacks of natural enzyme (GOx), such as high cost, difficult storage and low stability, might limit its in-field applications and could be further replaced by some nanozymes to enhance the stability and sensitivity of this biosensor.

## CRediT authorship contribution statement

**Ruya Guo:** Conceptualization, Methodology, Data curation, Writing – original draft. **Li Xue:** Conceptualization, Methodology, Data curation, Formal analysis. **Nana Jin:** Data curation. **Hong Duan:** Formal analysis. **Miaoyun Li:** Supervision. **Jianhan Lin:** Conceptualization, Formal analysis, Supervision, Project administration, Funding acquisition, Writing – review & editing.

## Declaration of competing interest

The authors declare that they have no known competing financial interests or personal relationships that could have appeared to influence the work reported in this paper.

## Acknowledgments

The work was supported by National Natural Science Foundation of China (32071899) and Walmart Foundation (UA2020-154).

## Appendix A. Supplementary data

Supplementary data to this article can be found online at https://doi.org/10.1016/j.bios.2022.114458.

## References

Bayareh, M., Ashani, M.N., Usefian, A., 2020. Active and passive micromixers: a comprehensive review. Chem. Eng. Process. Process Intensif. 147, 107771.
Cai, G., Xue, L., Zhang, H., Lin, J., 2017. A review on micromixers. Micromachines 8 (9).
Chen, Y., Xianyu, Y., Wu, J., Dong, M., Zheng, W., Sun, J., Jiang, X., 2017. Double-enzymes-mediated bioluminescent sensor for quantitative and ultrasensitive point-of-care testing. Anal. Chem. 89 (10), 5422–5427.
Harper, J.C., Andrews, J.M., Ben, C., Hunt, A.C., Murton, J.K., Carson, B., Bachand, G., Lovchik, J.A., Arndt, W.D., Finley, M.R., 2016. Magnetic-adhesive based valves for microfluidic devices used in low-resource settings. Lab Chip, 10.1039. C1036LC00858E.
Hussain, M., Liu, X., Tang, S., Zou, J., Wang, Z., Ali, Z., He, N., Tang, Y., 2022. Rapid detection of *Pseudomonas aeruginosa* based on lab-on-a-chip platform using immunomagnetic separation, light scattering, and machine learning. Anal. Chim. Acta 1189, 339223.
Iseri, E., Biggel, M., Goossens, H., Moons, P., van der Wijngaart, W., 2020. Digital dipstick: miniaturized bacteria detection and digital quantification for the point-of-care. Lab Chip 20 (23), 4349–4356.
Kim, H.J., Choi, S.J., 2020. Rapid single-cell detection of pathogenic bacteria for in situ determination of food safety. Anal. Methods 12 (46), 5621–5627.
Lee, C.-Y., Fu, L.-M., 2018. Recent advances and applications of micromixers. Sensor. Actuator. B Chem. 259, 677–702.
Liu, D., Zhang, Y., Zhu, M., Yu, Z., Ma, X., Song, Y., Zhou, S., Yang, C., 2020. Microfluidic-integrated multicolor immunosensor for visual detection of HIV-1 p24 antigen with the naked eye. Anal. Chem. 92 (17), 11826–11833.
Liu, J., Geng, Z., Fan, Z., Liu, J., Chen, H., 2019. Point-of-care testing based on smartphone: the current state-of-the-art (2017–2018). Biosens. Bioelectron. 132, 17–37.
Liu, Y., Tan, Y., Fu, Q., Lin, M., He, J., He, S., Yang, M., Chen, S., Zhou, J., 2021. Reciprocating-flowing on-a-chip enables ultra-fast immunobinding for multiplexed rapid ELISA detection of SARS-CoV-2 antibody. Biosens. Bioelectron. 176, 112920.
Meng, X., Li, F., Li, F., Xiong, Y., Xu, H., 2017. Vancomycin modified PEGylated-magnetic nanoparticles combined with PCR for efficient enrichment and detection of *Listeria monocytogenes*. Sensor. Actuator. B Chem. 247, 546–555.
Ming, T., Luo, J., Liu, J., Sun, S., Xing, Y., Wang, H., Xiao, G., Deng, Y., Cheng, Y., Yang, Z., Jin, H., Cai, X., 2020. Paper-based microfluidic aptasensors. Biosens. Bioelectron. 170, 112649.
Nishat, S., Jafry, A.T., Martinez, A.W., Awan, F.R., 2021. Paper-based microfluidics: simplified fabrication and assay methods. Sensor. Actuator. B Chem. 336, 129681.
Pang, B., Fu, K., Liu, Y., Ding, X., Hu, J., Wu, W., Xu, K., Song, X., Wang, J., Mu, Y., Zhao, C., Li, J., 2018. Development of a self-priming PDMS/paper hybrid microfluidic chip using mixed-dye-loaded loop-mediated isothermal amplification assay for multiplex foodborne pathogens detection. Anal. Chim. Acta 1040, 81–89.
Park, J., Han, D.H., Hwang, S.H., Park, J.K., 2020. Reciprocating flow-assisted nucleic acid purification using a finger-actuated microfluidic device. Lab Chip 20.
Park, J., Park, J.K., 2019. Finger-actuated microfluidic display for smart blood typing. Anal. Chem. 91 (18), 11636–11642.
Raza, W., Hossain, S., Kim, K.-Y., 2020. A review of passive micromixers with a comparative analysis. Micromachines 11 (5), 455.
Rocca, M., Temiz, Y., Salva, M.L., Castonguay, S., Gervais, T., Niemeyer, C.M., Delamarche, E., 2021. Rapid quantitative assays for glucose-6-phosphate dehydrogenase (G6PD) and hemoglobin combined on a capillary-driven microfluidic chip. Lab Chip 21 (18), 3573–3582.
Ting-Hang, Liu, Shu, Shen, Cheng, Huey, Ling, You, Mel, S., Lee, Gwo-Bin, 2019. Bacterial detection and identification from human synovial fluids on an integrated microfluidic system. Analyst 144 (4), 1210–1222.
Um, M.M., Castonguay, M.H., Mahamad Amine, K., Giguere, J., Morin, I., Dufour, S., 2020. Repeatability of a commercially available ELISA test for determining the herd-level *Salmonella enterica subsp. enterica* serovar dublin status in dairy herds using bulk milk. Front. Vet. Sci. 7, 401.
Venzac, B., Liu, Y., Ferrante, I., Vargas, P., Yamada, A., Courson, R., Verhulsel, M., Malaquin, L., Viovy, J.L., Descroix, S., 2020. Sliding walls: a new paradigm for fluidic actuation and protocol implementation in microfluidics. Microsyst. Nanoeng. 6, 18.
Wang, Z., Cai, R., Gao, Z., Yuan, Y., Yue, T., 2020. Immunomagnetic separation: an effective pretreatment technology for isolation and enrichment in food microorganisms detection. Compr. Rev. Food Sci. Food Saf. 19 (6), 3802–3824.
Xing, G., Zhang, W., Li, N., Pu, Q., Lin, J.-M., 2021. Recent progress on microfluidic biosensors for rapid detection of pathogenic bacteria. Chin. Chem. Lett.
Yakoh, A., Chaiyo, S., Siangproh, W., Chailapakul, O., 2019. 3D capillary-driven paper-based sequential microfluidic device for electrochemical sensing applications. ACS Sens. 4 (5), 1211–1221.
Yang, A.-S., Chuang, F.-C., Chen, C.-K., Lee, M.-H., Chen, S.-W., Su, T.-L., Yang, Y.-C., 2015. A high-performance micromixer using three-dimensional Tesla structures for bio-applications. Chem. Eng. J. 263, 444–451.
Zhang, D., Li, C., Ji, D., Wang, Y., 2021. Paper-based microfluidic sensors for onsite environmental detection: a critical review. Crit. Rev. Anal. Chem. 1–40.